Residual stress analysis of butt welds made of additively and traditionally manufactured 316l stainless steel plates

Jan Schubnell, Ardeshir Sarmast, Felix Altenhöner, Shahram Sheikhi, Moritz Braun, Sören Ehlers

RESIDUAL STRESS ANALYSIS OF BUTT WELDS MADE OF ADDITIVELY AND TRADITIONALLY MANUFACTURED 316L STAINLESS STEEL PLATES

Jan Schubnell [a, *], Ardeshir Sarmast [a], Felix Altenhöner [b], Shahram Sheikhi [b], Moritz Braun [c], Sören Ehlers [c, d]

[a] *Fraunhofer Institute for Mechanics of Materials, Woehlerstr. 11, Freiburg, Germany*
[b] *University of Applied Science Hamburg, Institute of Materials Science and Joining Technology, Berliner Tor 13, D-20099 Hamburg, Germany*
[c] *Hamburg University of Technology, Institute of Ship Structural Design and Analysis, Am Schwarzenberg-Campus 4C, D-21073 Hamburg, Germany*
[d] *German Aerospace Centre (DLR), Institute of Maritime Energy Systems, Max-Planck-Straße 2, D-21502 Geesthacht, Germany*

ABSTRACT

Due to the limited building volume of powder bed additive manufactured (AM) methods, combining several AM parts for a larger part through a welding joint may be required. Through AM processes, Laser powder bed fusion (LPBF) has a great potential because it enables the production of nearly full-density components. But the residual stresses are still an issue in the wide application of this method. In this study residual stress analysis of butt joints made of 316L AM steel plates compared to conventional rolled steel plates were performed by X-ray diffraction with two different analysis methods: The commonly used $\sin^2\psi$-method and the comparably new $\cos\alpha$-method. Complex residual stress states were determined at the welds made of AM steel plates compared to the welds made of conventional steel plates. High tensile residual stresses were determined in the AM plates depending on the layer orientation, but high compressive residual stresses were measured in the rolled steel plates. However, the residual stress level in the heat affected zone (HAZ) of the weld was comparably low in the AM steel plates and similar to the welds made of rolled steel plates. The residual stress analysis with the $\cos\alpha$-method showed the advantage of the comparable short measurement time based on small radiation time compared to the conventional $\sin^2\psi$-method. A high influence of the layer orientation and manufacturing process was determined on the residual stress state at the base material. Close to the weld, relatively small differences in residual stress state between the investigated conditions were measured by both methods.

Keywords: Residual stress, Additive Manufacturing, Gas metal arc welding, $\cos\alpha$-method, $\sin^2\psi$-method

1. Introduction

AM and LPBF has seen a rapid increase in application for many applications in recent years; however, there are still limitation with respect to widespread industrial applications. One important aspect is the joining of different additively manufactured parts or combinations with traditionally manufactured components such as wrought materials [1]. Welding of AM parts is thought to be an attractive option to join AM parts to larger structures, but there are currently only a few investigations on the mechanical properties of welded AM parts and compared to

* Jan Schubnell. jan.schubnell@iwm.fraunhofer.de

welded joints of wrought material. The reason for the unknown influence is related to the interaction of additional welding-related heat input and properties of the AM parts, including surface topology, microstructure, imperfections and residual stress states [2].

Previous investigations have shown that the LPBF process of 316L steel is always accompanied by the induction of residual stresses depending on the process parameters [3]. Furthermore, fatigue strength of 316L steel welds are strongly related to their residual stresses [4]. Tensile residual stress forms in the longitudinal direction after deposition of the material [5]. In the case of powder bed fusion additive manufacturing these residual stresses could be as high as the bulk material yield strength or even excessive of that [6]. For this reason, several researchers studied the formation of the residual stresses on macro- and micro-scale. Guo et al. [7] studies fluctuations in local residual stresses in direct energy deposited 316L. Wu et al. [6] in another work investigated the effect of AM process parameters and component geometry on the residual stress formation on the surface of the additively manufactured 316L specimens and showed that the residual stresses are compressive in depth of an additive manufacturing 316L component and tensile near its surface.

Based on the mentioned investigations it is assumed that the residual stress state affects the fatigue life of welded joints made of conventionally hot rolled and LPBF 316L steel sheets. Furthermore, the interaction between welding residual stresses and the stress state of the steel sheets after hot rolling or LPBF is unknown. The aim of this study is to quantify the residual stress state after welding depending on the manufacturing process of the base material.

2. Specimen and manufacturing

For this study, 316L steel was used in different conditions (powder, hot rolled steel sheets and filler material for welding). The chemical compositions are given in Table 1. Mechanical properties of the wrought material and for similar AM parameters were given by Braun et al. [8]. LPBF plates were built on a Renishaw AM 250 system. The dimensions were 140 mm in length and height with a thickness of 4 mm. The plates were manufactured perpendicular to the base plate. The scanning strategy used a rotation by 67° in the scanning direction after each layer. During the building process the chamber was filled with argon as shielding gas. The manufacturing parameters and the LPBF plates after manufacturing are displayed in Table 2 and Figure 1(a), respectively. For each specimen, four plates were combined by welding, see Figure 1(b).

Table 1. Chemical composition of the base metals and wire (wt%)

	Cr	Ni	Mo	Mn	Si	C	N	Nb	P	Fe
LPBF 316L	16.77	11.98	2.27	0.90	0.55	0.015	0.070	0.011	0.009	67.22
Hot rolled 316L	16.85	9.63	1.89	1.21	0.28	0.016	0.041	0.027	0.017	69.36
Wire 316LSi	18.65	11.64	2.29	1.76	0.65	0.026	0.035	0.016	0.003	64.62

Before welding the plates were prepared in a Y-shape with a 45-degree and 1 mm chamfer. The edge faces of the LPBF and hot rolled plates were ground (P320) between the butt welds. Afterwards the area for the welding was cleaned with acetone. Gas metal arc welding (GMAW) was performed in pulse mode with a Dinse DIX PI 400. For even welding seams, the torch was assembled on an automated gantry system. The same parameters were used for all welds, which are displayed in Table 3. The base metals and welded cross-sections were assessed using stereomicroscopy. The results are presented Figure 2.

Table 2. LPBF manufacturing parameters

Parameter	Unit	Value
Laser power	[W]	200
Laser scanning speed	[mm/s]	812.5
Layer thickness	[µm]	40
Hatching Distance	[µm]	110
Scanning pattern	[-]	Strips

Table 3. GMAW welding parameters

Parameter	Unit	Value
Arc current	[A]	122
Voltage	[V]	21.5
Wire feed rate	[m/min]	7.8
Wire diameter	[mm]	1
Torch angle	[deg]	0
Travel speed	[mm/min]	600
Standoff distance	[mm]	10

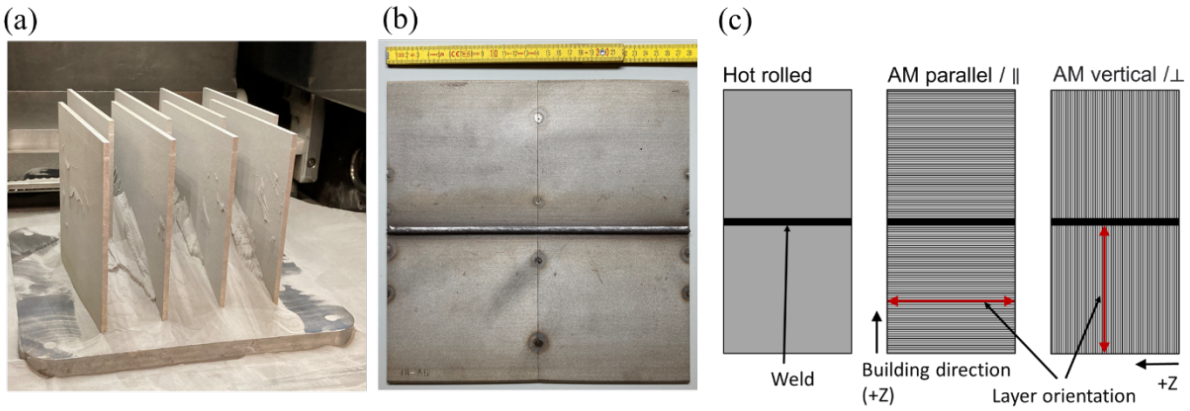

Figure 1. (a) LPBF manufacturing of plates; (b) Specimens joined from four LPBF plates; (c) Investigated conditions.

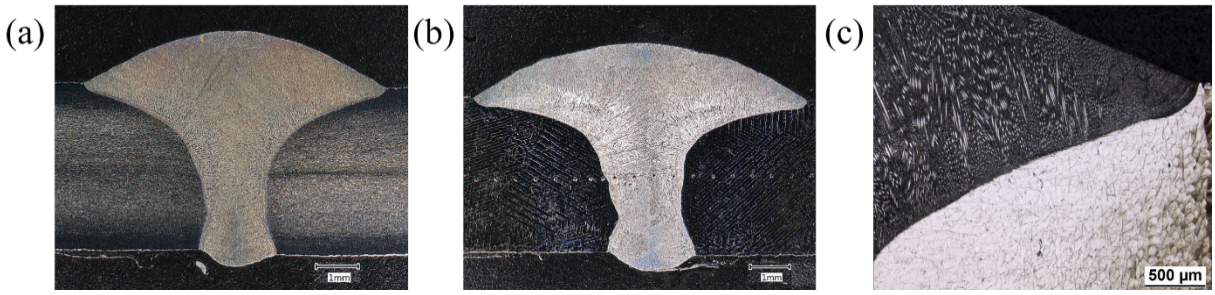

Figure 2. (a) Hot rolled plate: macrograph of the weld seam; (b) LPBF plate: macrograph of the weld seam and hardness measurements; (c) Magnification of fusion zone, HAZ and base metal (AM).

3. Residual stress analysis

3.1. Sin²ψ-method

Residual stresses can be determined by X-ray diffraction. Residual stresses change the lattice spacing of an unstrained crystal. According to Bragg's law, a decrease or increase in the lattice spacing appears as the angular shift in position of the diffraction line. After determining the position of the diffraction line 2θ at the tilt angel ψ, the residual stresses are calculated according to the theory of the elasticity and the slope of the 2θ-$\sin^2\psi$ diagram (equation (1)). For polycrystalline materials, $\sin^2\psi$-method [9] has been widely used. Corresponding formulations for the calculation of the strain and stress in a given direction are as below [10], [11]:

$$\frac{d_\psi - d_0}{d_0} = \frac{1+\nu}{E}\sigma_\phi Sin^2\psi - \frac{\upsilon}{E}(\sigma_{11}+\sigma_{22}) \quad (1)$$

$$\sigma_\phi = \frac{E}{(1+\upsilon)Sin^2\psi}\left(\frac{d_\psi - d_n}{d_n}\right) \quad (2)$$

Figure 3(a) shows the schematic representation of the system that above equations are in.

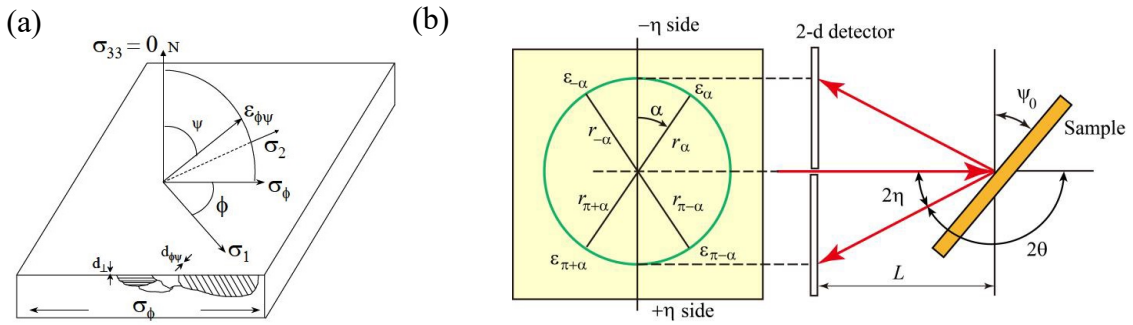

Figure 3. (a) Schematic representation of the diffraction planes for the evaluation with the sin²ψ-method [11], (b) Principle of stress analysis by the cosα-method [12].

In equation (2), d_0 is replaced with d_n which is the lattice spacing of ψ=0. It is the main advantage of the sin²ψ-method that we can replace the strain-free lattice spacing (d0), which is difficult to obtain, with d_ψ=0 without a significant error as the d_0 value is a multiplier to the slope of the 2θ-sin²ψ curve [10]. Zero-dimensional and one-dimensional detector are normally used for the measurements in this method.

For the aim of this study a D8 Discover laboratory x-ray diffractometer was used. Cr-K$_\alpha$ radiation was utilized to target {311} planes at 2θ=128.8°. The beam diameter was 1mm with a 1.2 kW power. One dimensional Lynxeye XE-T detector was used for the data collection. Data collection time was 2 sec, and the step size was 0.04°.

3.2. Cosα-method

The stress analysis by the cosα-method according to Taira [13] is based on a strain evaluation over the complete Debye-Scherrer-ring based on a 2D-detector (digital image plate). The reliability of this method in combination with the 2D-detector compared to the commonly used sinψ²-method [14] was achieved by Sasaki et al [15], [16] for austenitic stainless steels. The strain in circumferential direction is measured by a shift of the diffraction angle θ_α or radius r_α depending on the α-position on the detector, shown in Figure 3(b). For the measurement detector distance to specimen L and tilt angle ψ_0 is constant. A strain parameter ε_{a1} is defined based on four strains from α=0° to 90°. The stress σ_ϕ is calculated according to equation (3) and equation (4). A detailed description of the method was published by Tanaka [12].

$$\sigma_\phi = -\frac{E}{1+\upsilon}\frac{1}{2\,sin\,\eta\,sin\,2\psi_0}\frac{\delta\varepsilon_{a1}}{\delta\,cos\,\alpha} \quad (3)$$

$$\text{with } \varepsilon_{\alpha 1} = [(\varepsilon_\alpha - \varepsilon_{\pi+\alpha}) + (\varepsilon_{-\alpha} - \varepsilon_{\pi-\alpha})]/2 \quad (4)$$

For the XRD-analysis by the cosα-method a diffractometer type Pulstec μ-360 were used. The diffractometer was mounted on an industrial robot type Kuka KR3 R540. A sample distance of L=37 mm and a tilt angle of ψ_0=30° were used for the measurement. Due to coarse grain effects a linear oscillation in Y-direction by ±2.5 mm was implemented, like the measurements by the sin²ψ-method. The measurement parameters of both methods are summarized in Table 4.

Table 4. Parameter for XRD-analysis

Parameter	Radiation	Lattice plane	E [GPa]	ν [-]	$\emptyset$ [mm]	Exposure time	Measurement time
$\sin^2\psi$-method	Cr-K_α	{311}	189	0.29	1	2.5h	≈3h
Cosα-method	Cr-K_β	{220}				60s	≈120s

3.3. Results

Residual stress measurements (cosα-method) were performed in distance of 20 mm over the complete specimen of each condition (hot rolled, AM vertical, AM parallel) to quantify the residual stress state at the base material, illustrated in Figure 4. It is assumed that the residual stresses in a distance of 30 mm to the weld are unaffected from the weld process. The residual stresses in transverse and longitudinal direction shows high differences from the edge of the specimen to the weld and is not constantly distributed over the specimen length. In AM parallel condition, tensile residual stresses up to 210 MPa were determined in transverse direction. These were of similar value as the determined longitudinal residual stresses in AM vertical condition (transverse). Thus, measurements on both sides of the specimen in hot rolled direction showed compressive residual stresses in transverse and longitudinal directions between 150 MPa and 280 MPa.

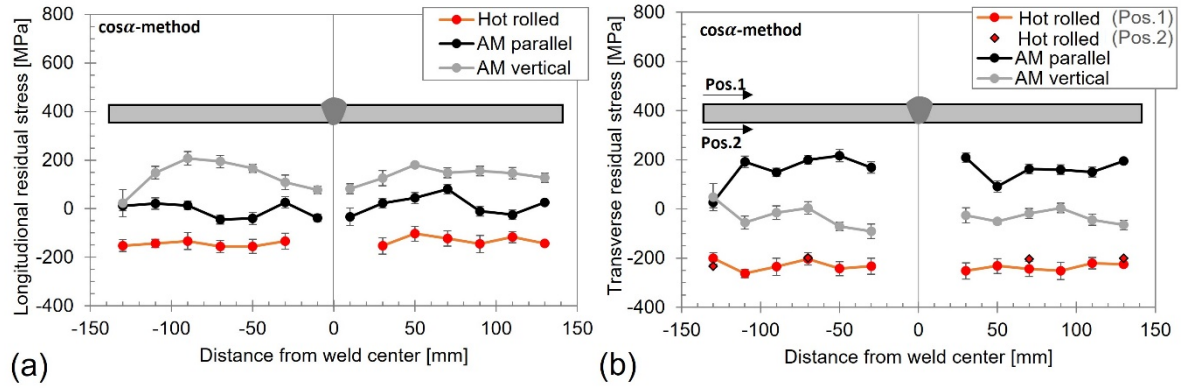

Figure 4. (a) Longitudinal and (b) Transverse residual stress distribution over the complete specimen.

The residual stress distribution at the center of the specimen around the weld is given in Figure 5. The measurements were performed with the cosα-method and $\sin^2\psi$-method. The error bar in the graphs represents the standard deviation taken from the cosα- and $\sin^2\psi$-distribution. All measurements were performed on a single line at the center of the specimen. Close to the weld toe comparable low residual stresses values between -75 MPa and 25 MPa were determined for both AM conditions in transverse direction. In hot rolled condition tensile residual stresses between 30 MPa and 110 MPa were measured in longitudinal direction. However, only compressive residual stresses could be determined in transverse direction in hot rolled condition. The residual stress state shows significantly less differences in all three conditions compared to the measurements of the base material, shown in Figure 4. No significant texture effect could be determined by the used measurements methods for all material conditions. The distribution of the full width half maximum, see Figure 5, shows nearly no differences for both AM conditions.

Compared to the $\sin^2\psi$-method, the cosα-method shows a significantly higher standard deviation (between 4 to 6 times higher). The maximum difference between the two methods was 60 MPa. However, both methods generally show a similar residual stress distribution for each investigated material condition. Furthermore, the measurement time according to the cosα-method with a lower intensity Cr-K_β radiation was significantly lower compared to the $\sin^2\psi$-method.

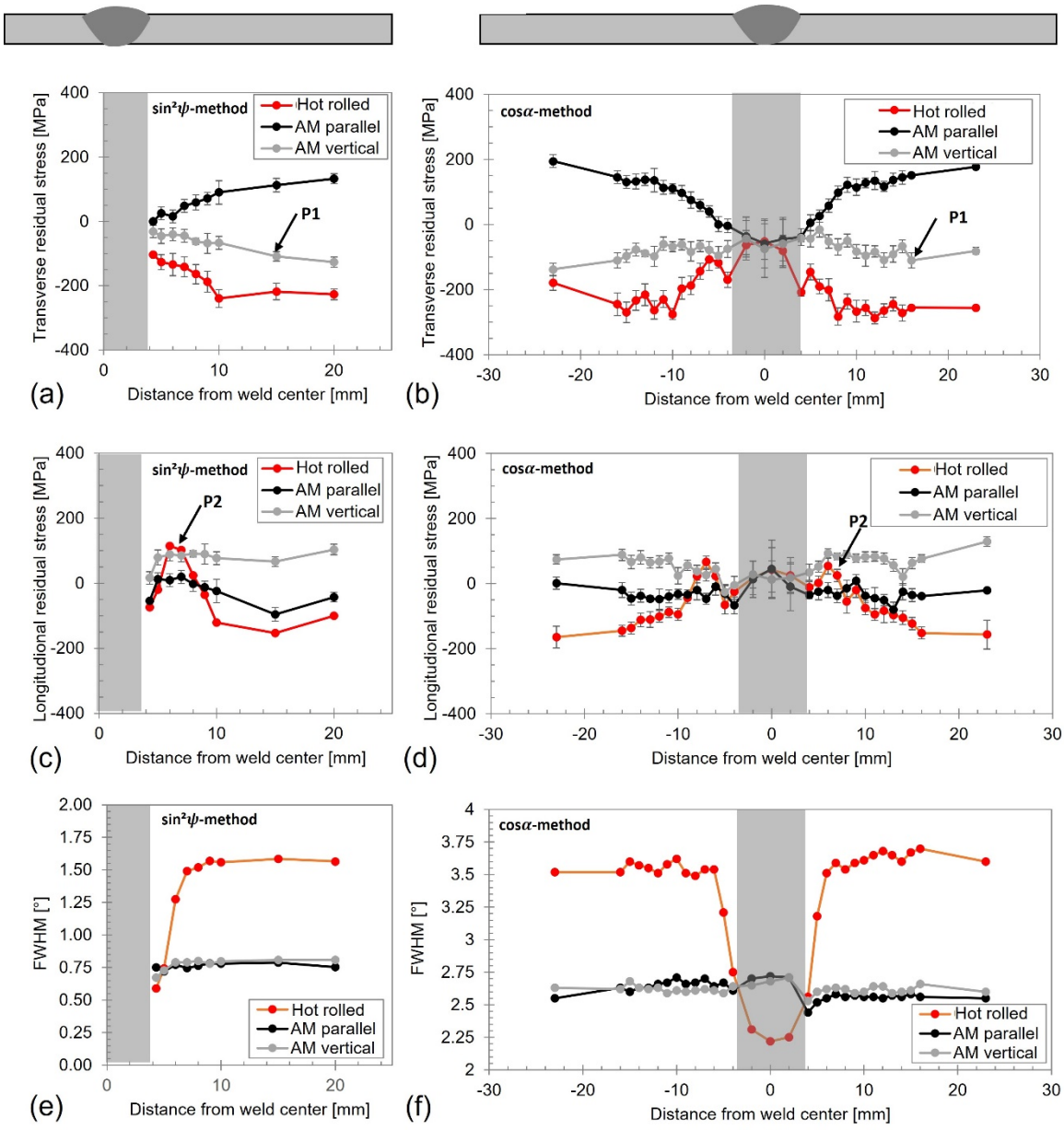

Figure 5. Residual stress distribution in the weldments depending on the material condition.

For further analysis of the deviation of $\sin^2\psi$- and $\cos\alpha$-method, two representative measurements were compared in detail: Point 1 (AM vertical) in a distance of 15 mm from the weld toe that shows a good agreement with both methods and point 2 (hot rolled condition) that shows a high difference between both methods, see Figure 5(a), (b), (c) and (d). As illustrated, in both measurements there are high deviations in the $\cos\alpha$-distribution and no significant texture effect or shear stress is shown in the $\sin^2\psi$-distribution. However, in hot rolled condition, see Figure 6(b), gaps and deviations in the $\cos\alpha$-distribution lead to high standard deviation according to a linear fitting procedure.

4. Discussion

The measurements reveal a high influence of the AM direction on the results stress state at the base material. Tensile residual stresses in loading direction may affect the fatigue behavior. Fatigue tests should prove if there is still an effect of the building direction on the fatigue strength of the specimen. This is the case for the specimen in AM vertical condition. However,

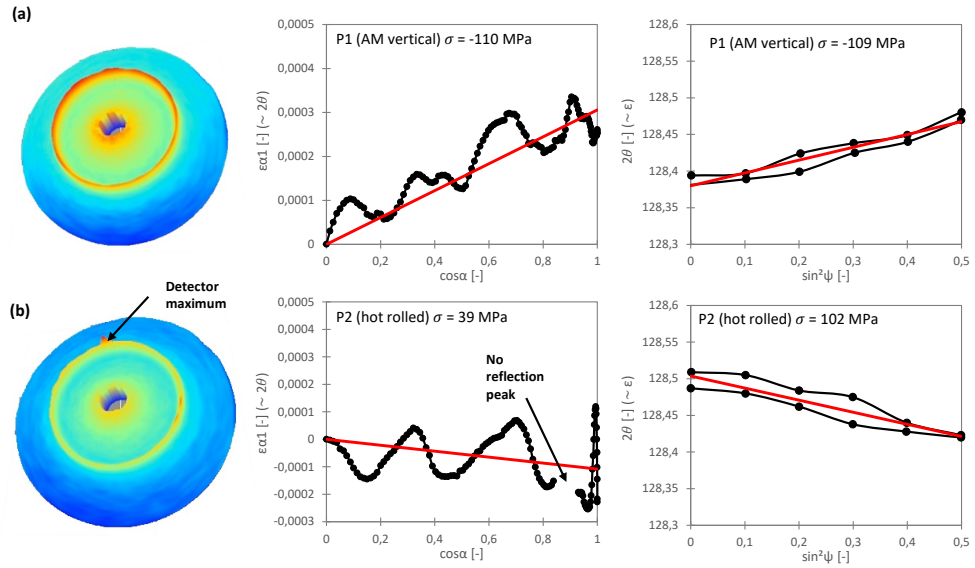

Figure 6. Debye-Scherrer ring, cosα- and sin²ψ-distribution for two representative measurement points.

it seems that the welding process releases these harmful tensile residual stresses around the weld toe. Further fatigue tests should prove if there is still an effect of the building direction on the fatigue strength of the specimen.

Both measurements sin²ψ- and cosα-method showed comparable residual stress distributions. However, especially in hot rolled conditions higher deviations between the two measurements methods could be perceived. Possible error sources are the different detector resolution and radiation used for the measurements. Coarse grain effects lead to gaps in the cosα-distributions and may affect the evaluated residual stress values, see Figure 6 (b). Linear oscillation of the diffractometer led to better results. However, especially close to the weld toe the highest deviations between the two methods were determined in hot rolled condition and longitudinal direction. It is assumed that coarse grains in the heat affected zone may be the reason for this deviation. The usage of V-K_α radiation or Mn-K_α radiation, also recommended by Sasaki [15], could lead to a better result for the cosα-method. The higher number of evolution points for the cosα-alpha method (α-resolution of 0.72° leads to 500 points) may also explain the high standard deviation compared to the sin²ψ-method with 24 points e.g. ψ-angles per measurement.

5. Conclusion

Gas metal arc welding (GMAW) of 316L steel sheets made by laser power bed fusion (LPBF) and hot rolling was performed to investigate the possibility to combine several additive manufactured (AM) parts due to a limited building volume. The residual stress state after welding was investigated by X-ray diffraction analysis (XRD) by the sin²ψ-method and cosα-method. Three base material conditions after welding were investigated: Hot rolled steel plates, AM steel plates in vertical and horizontal building direction. The XRD analysis by both methods show a good agreement. However, higher deviation could be determined between sin²ψ- and cosα-method at some single points, especially for the measurement at specimen in hot rolled condition close to the weld due to the coarse grain effect. Regarding the evaluated residual stress (RS) state at the investigated welded joints following conclusion can be made:

- The residual stress state (tensile RS in AM condition, compressive RS in hot rolled condition) is not constantly distributed over the specimen. The layer orientation of the base plates before welding may affect the residual stress state after welding.

- The building direction has a high influence on the residual stress state. In the building direction significantly higher tensile RS are determined compared to perpendicular to the building direction.
- In the AM condition, welding influences the RS state, leads to relaxation of the tensile RS close to the weld. This results in similar RS states regardless of the base material condition.

In the next step fatigue tests will be performed, accompanied by residual stress measurements after loading. The information about the relaxation of the residual stress under cyclic loading is assumed to be important to quantify the influence of the residual stresses on the fatigue behavior of welded AM parts and components.

References

[1] H. Zapf, M. Höfemann, and C. Emmelmann, "Laser welding of additively manufactured medium manganese steel alloy with conventionally manufactured dual-phase steel" *Procedia CIRP*, vol. 94, pp. 655–660, Jan. 2020, doi: 10.1016/J.PROCIR.2020.09.102.

[2] B. Möller, K. Schnabel, M. Scurria, A. Jöckel, and J. Baumgartner, "Fatigue assessment of laser beam welds between AlSi10Mg AM-structures and conventionally manufactured aluminum by local approaches" *Procedia Struct. Integr.*, vol. 34, pp. 160–165, Jan. 2021, doi: 10.1016/J.PROSTR.2021.12.023.

[3] T. Simson, A. Emmel, A. Dwars, and J. Böhm, "Residual stress measurements on AISI 316L samples manufactured by selective laser melting" *Addit. Manuf.*, vol. 17, pp. 183–189, Oct. 2017, doi: 10.1016/J.ADDMA.2017.07.007.

[4] W. Jiang *et al.*, "Fatigue life prediction of 316L stainless steel weld joint including the role of residual stress and its evolution: Experimental and modelling" *Int. J. Fatigue*, vol. 143, p. 105997, Feb. 2021, doi: 10.1016/J.IJFATIGUE.2020.105997.

[5] M. Abbaszadeh *et al.*, "Numerical Investigation of the Effect of Rolling on the Localized Stress and Strain Induction for Wire + Arc Additive Manufactured Structures" *J. Mater. Eng. Perform.*, vol. 28, no. 8, pp. 4931–4942, 2019.

[6] A. S. Wu, D. W. Brown, M. Kumar, G. F. Gallegos, and W. E. King, "An Experimental Investigation into Additive Manufacturing-Induced Residual Stresses in 316L Stainless Steel" *Metall. Mater. Trans. A Phys. Metall. Mater. Sci.*, vol. 45, no. 13, pp. 6260–6270, 2014, doi: 10.1007/s11661-014-2549-x.

[7] D. Guo *et al.*, "Solidification microstructure and residual stress correlations in direct energy deposited type 316L stainless steel" *Mater. Des.*, vol. 207, p. 109782, 2021, doi: 10.1016/j.matdes.2021.109782.

[8] M. Braun *et al.*, "Fatigue strength of PBF-LB/M and wrought 316L stainless steel: effect of post-treatment and cyclic mean stress" *Fatigue Fract. Eng. Mater. Struct.*, vol. 44, no. 11, pp. 3077–3093, Nov. 2021, doi: 10.1111/FFE.13552.

[9] E. Macherauch and P. Müller, "Das Sin^2ψ Verfahren von Rontgenographische Eigenspannungen" *Z. angew. Phys.*, vol. 13, pp. 305–312, 1961.

[10] P. J. Withers, "Residual stress and its role in failure" *Reports Prog. Phys.*, vol. 70, no. 12, pp. 2211–2264, 2007, doi: 10.1088/0034-4885/70/12/R04.

[11] M. E. Fitzpatrick, A. T. Fry, P. Holdway, F. A. Kandil, J. Shackleton, and L. Souminen, "NPL Good Practice Guide no . 52 : determination of residual stresses by x-ray diffraction Determination of Residual Stresses by X-ray Diffraction - Issue 2" 2002.

[12] K. Tanaka, "The cosα method for X-ray residual stress measurement using two-dimensional detector" *Mech. Eng. Rev.*, vol. 6, no. 1, pp. 18-00378-18–00378, 2019, doi: 10.1299/mer.18-00378.

[13] S. Taira, K. Tanaka, and T. Yamasaki, "A Method of X-Ray Microbeam Measurement of Local Stress an Its Application to Fatigue Crack Growth Problems" *J. Soc. Mater. Sci.*, vol. 27.294, pp. 251–256, 1978.

[14] P. Müller and E. Macherauch, "Das sin 2 ψ-Verfahren der röntgenographischen Spannungsmessung" *Z. angew. Phys*, vol. 13, pp. 305–312, 1961.

[15] T. Sasaki and H. Sato, "X-ray stress measurement of austenitic stainless steel with cosα method and two-dimensional X-ray detector" in *Materials Science Forum*, 2017, vol. 879, pp. 1679–1684, doi: 10.4028/www.scientific.net/MSF.879.1679.

[16] T. Miyazaki and T. Sasaki, "X-ray residual stress measurement of austenitic stainless steel based on fourier analysis" *Nuclear Technology*, vol. 194, no. 1. American Nuclear Society, pp. 111–116, Apr. 01, 2016, doi: 10.13182/NT15-25.